Herschel Observations: Constraints on Dust Attenuation and Star Formation Histories at High Redshift

Denis Burgarella,[1] Véronique Buat,[1] Carlotta Gruppioni,[2] Olga Cucciati,[2] Sébastien Heinis,[1] and the PEP/HerMES Team

[1] *Aix-Marseille Université, CNRS, LAM (Laboratoire d'Astrophysique de Marseille), France*
[2] *INAF-Osservatorio Astronomico di Bologna, Italy*

ABSTRACT

SPICA is one of the key projects for the future. Not only its instrument suite will open up a discovery window but they will also allow to physically understand some of the phenomena that we still do not understand in the high-redshift universe. Using new homogeneous luminosity functions (LFs) in the Far-Ultraviolet (FUV) from VVDS and in the Far-Infrared (FIR) from *Herschel*/PEP and *Herschel*/HerMES, we studied the evolution of the dust attenuation with redshift. With this information, we are able to estimate the redshift evolution of the total (FUV + FIR) star formation rate density (SFRD$_{\rm TOT}$). Our main conclusions are that: 1) the dust attenuation $A_{\rm FUV}$ is found to increase from $z = 0$ to $z \sim 1.2$ and then starts to decrease until our last data point at $z = 3.6$; 2) the estimated SFRD confirms published results to $z \sim 2$. At $z > 2$, we observe either a plateau or a small increase up to $z \sim 3$ and then a likely decrease up to $z = 3.6$; 3) the peak of $A_{\rm FUV}$ is delayed with respect to the plateau of SFRD$_{\rm TOT}$ but the origin of this delay is not understood yet, and *SPICA* instruments will provide clues to move further in the physical understanding of this delay but also on the detection and redshift measurements of galaxies at higher redshifts. This work is further detailed in Burgarella et al. (2013).

1. INTRODUCTION

Over the past 15 years or so, astronomers have tried to measure the evolution of the cosmic star formation rate density (SFRD) moving higher and higher in redshift. However, we quickly understood that one of the main issues was to account for the total SFRD and not only for the far-ultraviolet (FUV) one. This means either a dust correction of the FUV SFRD or, better, a measure of the total i.e., FUV plus far-infrared (FIR = bolometric IR) SFRD. Knowing how the dust attenuation evolves in redshift is therefore mandatory if one wishes to study the redshift evolution of the SFRD.

Takeuchi et al. (2005) estimated the cosmic evolution of the SFRD from the FUV and FIR. An increase of the fraction of hidden SFR is found to $z = 1$ where it reaches ~84 %. The dust attenuation increases from $A_{\rm FUV} \sim 1.3$ mag locally to $A_{\rm FUV} \sim 2.3$ mag at $z = 1$. From the FUV only Cucciati et al. (2012) show that the mean dust attenuation $A_{\rm FUV}$ agrees with Takeuchi et al. (2005) over the range $0 < z < 1$, remains at the same level to $z \sim 2$, and declines to ~1 mag at $z \sim 4$.

Using FUV luminosity functions (LFs) published in Cucciati et al. (2012) and FIR LFs from *Herschel*[1] (Gruppioni et al. 2013), we are able to constrain the redshift evolution of $\log_{10}(L_{\rm FIR}/L_{\rm FUV})$ (aka IRX) to $z \sim 4$ for the first time directly from FIR data. With this information, we can estimate the redshift evolution of $\rho_{\rm FIR}/\rho_{\rm FUV}$ as well as $\rho_{\rm TOT} = \rho_{\rm FIR} + \rho_{\rm FUV}$.

The information gathered in this work poses a number of questions that would be addressed by *SPICA*. The physical study with *SPICA* of the high redshift galaxies detected by *Herschel* is crucial to better understand the formation and evolution of galaxies.

Throughout this paper we adopt a ΛCDM cosmology with $(H_0, \Omega_m, \Omega_\Lambda) = (70, 0.3, 0.7)$, where H_0 is in km s^{-1} Mpc^{-1}. All SFR and stellar masses presented assume, or have been converted to, a Salpeter IMF.

2. ABOUT LUMINOSITY FUNCTIONS

Figure 1 shows the redshift variation of the LFs in FIR. The known difference in the FIR and FUV LFs (e.g. Takeuchi et al. 2005) is clearly illustrated here: bright FIR galaxies are more numerous than bright FUV galaxies at $\log_{10}(L[{\rm L}_\odot]) > 10$. In the FUV, except in the highest redshift bins, $L^\star$ and $\Phi^\star$ remain approximately constant while the faint-end slope evolves. The FIR faint end slope is not observationally constrained at high z, and Gruppioni et al. (2013) fixed it to $\alpha = 1.2$. However, $L^\star$ and $\Phi^\star$ were allowed to change with redshift. These different evolutions of the FUV and FIR LFs are reflected in Figure 1 and explain the evolution of the cosmic SFRD and dust attenuation.

---

[1] From two *Herschel* Large Programmes: PACS Evolutionary Probe (PEP; Lutz et al. 2011) and the *Herschel* Multi-tiered Extragalactic Survey (HerMES; Oliver et al. 2012)
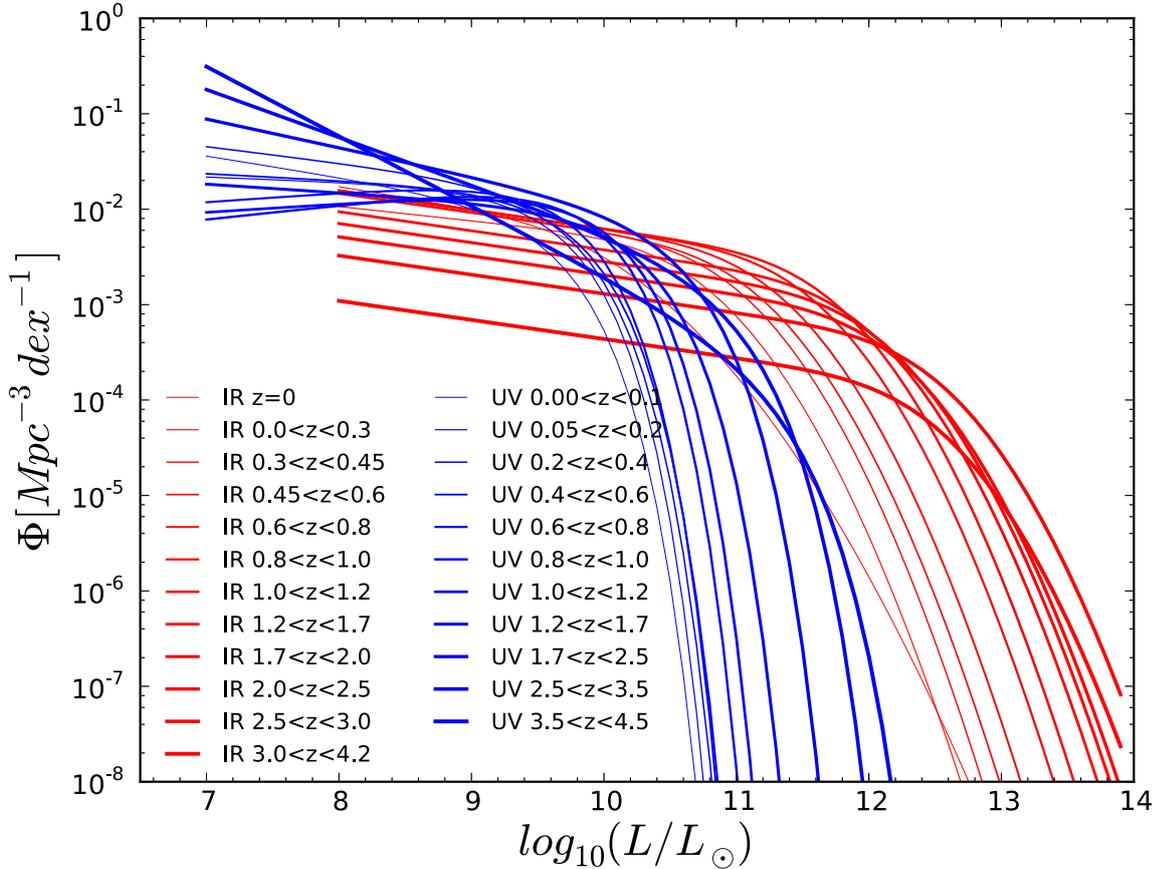
BURGARELLA ET AL.

Figure 1. Redshift evolution of the FIR (red, Gruppioni et al. 2013) and FUV (blue, Cucciati et al. 2012) LFs. Note that the FUV LFs are uncorrected for dust attenuation. The LFs at every other redshift are plotted in bold. The others are fainter to facilitate reading the figure. The LFs are plotted within the limits of integration.

3. ABOUT THE EVOLUTION OF THE COSMIC DUSTINESS

Figure 2 presents the dust attenuation in the FUV vs. z and the ratio of the FIR-to-FUV LDs integrated in the range $\log_{10}(L[L_\odot]) = [7, 14]$ in the FUV (i.e. $L_{\rm FUV}^{\rm min} = 1.65 \times 10^{-4} L_{z=3}^\star$, Bouwens et al. 2009) and [8, 14] in the FIR. The FUV dust attenuation is estimated from the IRX and converted to $A_{\rm FUV}$ using Burgarella et al. (2005)[2]. The redshift evolution of $A_{\rm FUV}$ agrees with Cucciati et al. (2012). Note that Cucciati et al. (2012) estimated $A_{\rm FUV}$ through an analysis of individual SEDs up to $\lambda_{\rm obs} = 2.2\,\mu m$ (Ks-band). Figure 2 suggests a local minimum at $z \sim 2$ that might be caused by UV-faint galaxies (see Figure 7 in Cucciati et al. 2012) that are responsible for a peak observed in the FUV LD that is not observed in the FIR. Since the fields observed in FUV and in FIR are not the same, another origin might be found in cosmic variance. The bottom line is that the existence of this trough in $A_{\rm FUV}$ must be explored with *SPICA*. Finally, higher redshift $A_{\rm FUV}$ from the UV slope, β, suggests a continuous decline at least to $z = 6$ (Bouwens et al. 2009).

We conclude that the cosmic dust attenuation $A_{\rm FUV}$ reaches an absolute maximum at $z \sim 1.2$ followed by a global decline to $z = 3.6$, where it reaches about the same level as measured at $z = 0$. Beyond $z = 4$, we do not expect any increase (e.g. Burgarella et al. 2005).

4. ABOUT THE TOTAL FUV+FIR STAR FORMATION DENSITY

Figure 3 suggests a flattening of the total SFRD up to $z \sim 3$ (as in Chary & Elbaz 2001; Le Floc'h et al. 2005; Franceschini et al. 2010; Goto et al. 2010; Magnelli et al. 2012), where the UV data favor a peak followed by a decrease. Note that we cannot rule out a small increase or decrease within the uncertainties. All in all, our total SFRD agrees fairly well with that of Hopkins & Beacom (2006) in the same redshift range. However, discrepancies exist: our total SFRD is lower at $z < 1$ and is only marginally consistent, but lower, at $z > 3$. Moreover, PACS data are less sensitive at higher than

---

[2] The conversion from IRX to $A_{\rm FUV}$ from Burgarella et al. (2005) is valid at $\log_{10}(L_{\rm FIR}/L_{\rm FUV}) > -1.2$: $A_{\rm FUV} = -0.028[\log_{10} L_{\rm FIR}/L_{\rm FUV}]^3 + 0.392[\log_{10} L_{\rm FIR}/L_{\rm FUV}]^2 + 1.094[\log_{10} L_{\rm FIR}/L_{\rm FUV}] + 0.546$
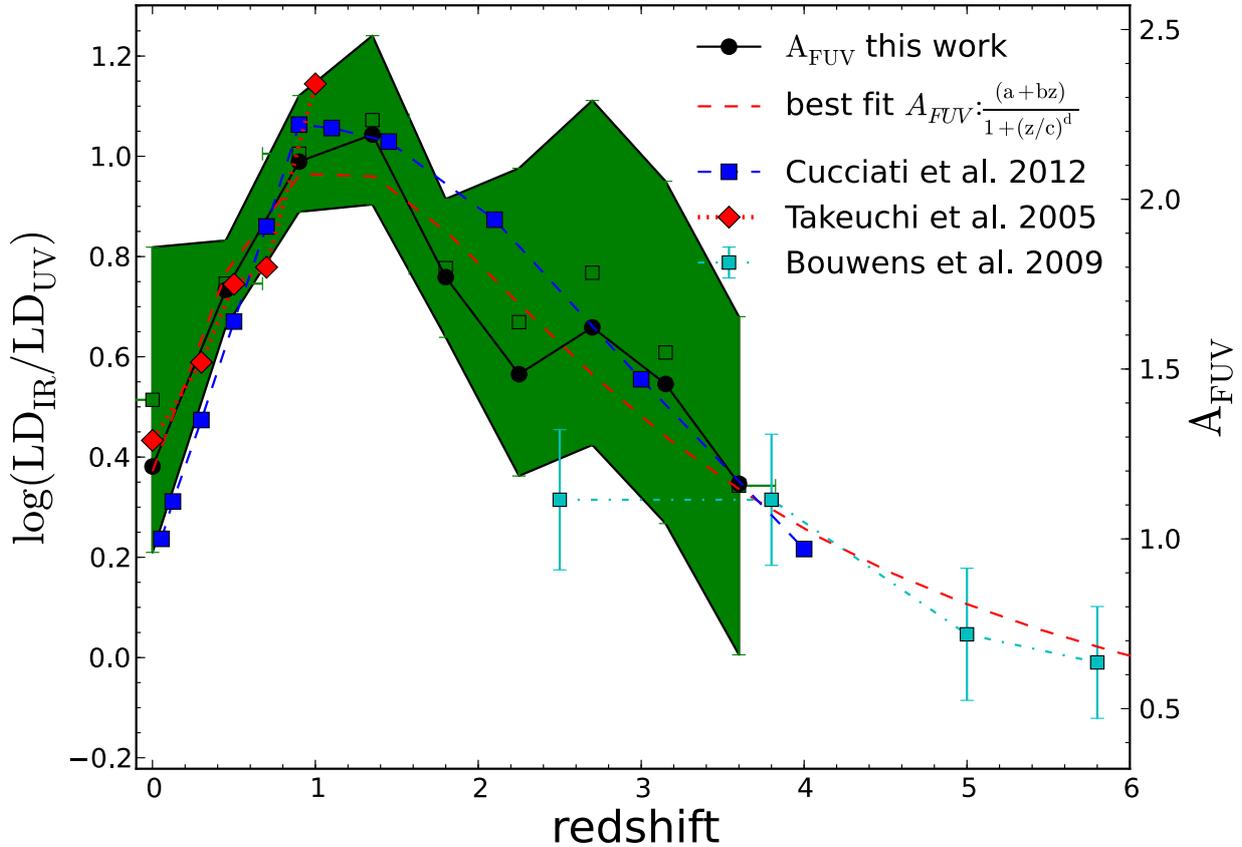
Figure 2. Left axis: ratio of the FIR-to-FUV LDs (*IRX*). Right axis: FUV dust attenuation (A_{FUV}). The red dotted line with red diamonds is taken from Takeuchi et al. (2005). The green filled area and green dots are the associated uncertainties estimated through bootstrapping with 2 000 drawings. Black dots denote the values directly computed from the LFs. At $z = 3.6$, A_{FUV} reaches about the same value as at $z = 0$. Takeuchi et al. (2005) (red diamonds) used an approach identical to ours while a SED analysis (no FIR data) is performed in Cucciati et al. (2012) (blue boxes). Bouwens et al. (2009) are estimates based on the UV slope β. The limiting FUV luminosity is $10^7\,L_\odot$ or $1.65 \times 10^{-4} L^\star_{z=3}$. The best fit is given by $A_{FUV}(z) = \frac{(a+bz)}{1+(z/c)^d}$ with $a = 1.20$, $b = 1.50$, $c = 1.77$, and $d = 2.19$.

at lower redshift because the rest-frame wavelength moves into the mid-IR. The preliminary FIR SFRD from Vaccari et al. (2013, in prep.) (*Herschel*/SPIRE selection) agrees excellently over the $0 < z \leq 2$ range, but is slightly higher than that derived from PACS at $z > 3$. However, this is only a $\sim 2\sigma$ difference. Barger et al. (2012) published a FIR SFRD based on SCUBA-2 data that also agrees with ours at $2 < z < 4$. We first tried to fit SFRD$_{TOT}$ with a one-peak analytical function (e.g. Hopkins & Beacom 2006; Behroozi et al. 2012), but the results are not satisfactory. So, we combined two Gaussians,

$$a_1 e^{\frac{-(z-z_1)^2}{2\sigma_1^2}} + a_2 e^{\frac{-(z-z_2)^2}{2\sigma_2^2}},$$

with $a_1 = 0.1261 \pm 0.0222$, $\sigma_1 = 0.5135 \pm 0.0704$, $z_1 = 1.1390 \pm 0.0959$ and $a_2 = 0.2294 \pm 0.0222$, $\sigma_2 = 0.8160 \pm 0.0964$, $z_2 = 2.7151 \pm 0.0839$. At higher redshifts, we made assumptions that are explained below.

The cosmic SFRD presents a (weak) maximum at $z \sim 2.5$–3.0 (i.e., between 2.6–2.1 Gyr) while the dust attenuation presents a maximum at $z \sim 1.2$ (i.e. 5 Gyr). We tried to lock the faint-end slope of the UV LF -1.2, to see how far out in redshift the obscuration peak could potentially move, but we detected no change, suggesting this effect is solid. We have no definite explanation for this delay of ~ 2.7 Gyr. Type II supernovae start producing dust earlier than AGB stars (e.g. Figure 3 in Valiante et al. 2009) but the difference in timescales is too short and only on the order of a few 10 Myr for the onset of dust formation. Dust grain destruction in the ISM might play a role (e.g. Dwek & Cherchneff 2011) but the efficiency of destruction is only poorly known and depends on the star formation history. These dust-related origins for the delayed maximum are unlikely. The best explanation might be that this delay is related to a global move of galaxies in the [$\log_{10}(L_{FIR}/L_{FUV})$ vs. $\log_{10}(L_{FIR} + L_{FUV})$] diagram. Buat et al. (2009) showed that galaxies evolve in redshift from $z = 0$ to $z = 2$ in this diagram, with high-redshift sources having lower *IRX* at given total luminosities.
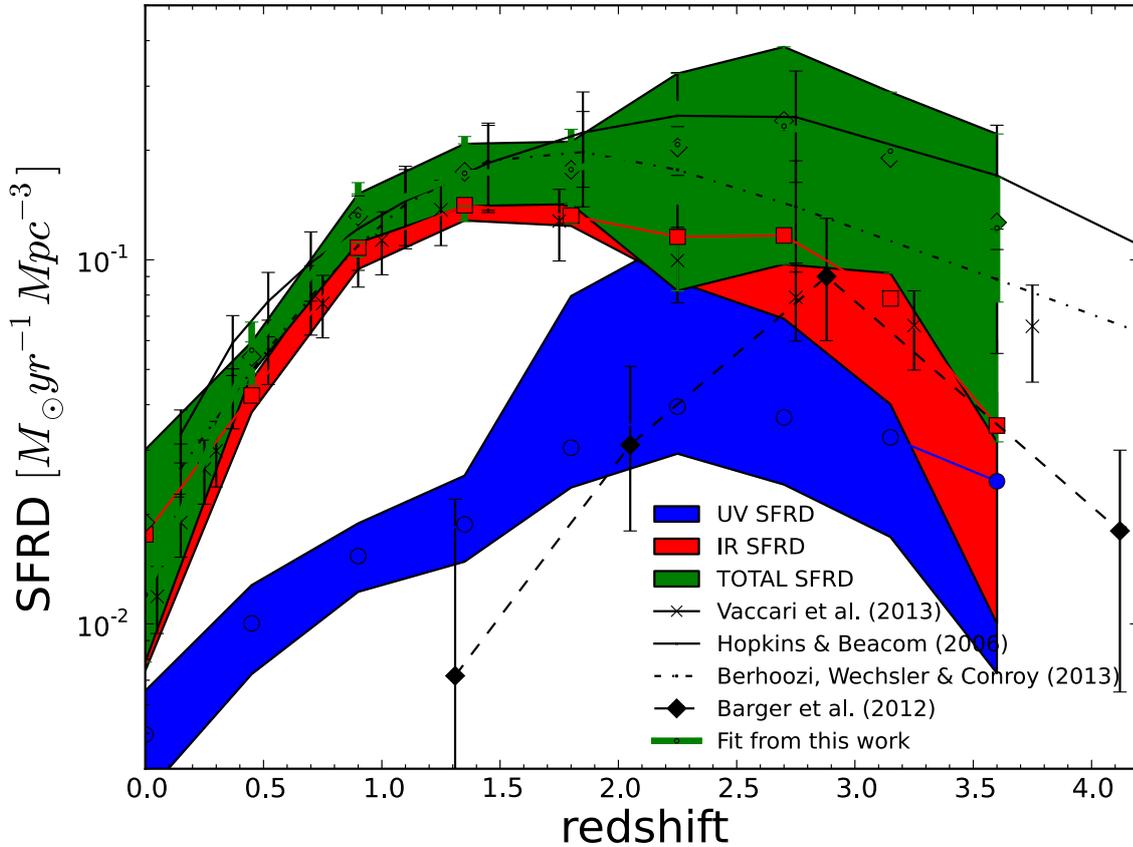
Figure 3. SFRD densities in the FUV (blue), in the FIR (red), and in total (i.e., FUV + FIR) in green (other colors are due to overlaps of the previous colors). The lines are the mean values, while the lighter colors show the uncertainties evaluated from the 2 000 runs as in Figure 2. After the initial increase of the total SFRD from $z = 0$ to $z \sim 1.2$, it remains flat or slightly increases/decreases up to $z \sim 2.5$–3.0 followed by a decrease. Globally and over $0 < z \le 3.6$, the total average SFRD is slightly below that reported in Hopkins & Beacom (2006) and agrees with that of Behroozi et al. (2012) up to $z \sim 2$. The SFRD from Barger et al. (2012) and preliminary results from *Herschel*/SPIRE estimated by Vaccari et al. (2013, in prep.) agree with these trends. Symbols and lines are explained in the plot.

5. CONCLUSIONS

On the one hand, the variation of the cosmic dust attenuation with redshift suggests a peak in the dust attenuation at $z \sim 1.2$ followed by a decline to $z = 3.6$. On the other hand, the total (FUV+FIR) cosmic SFRD increases from $z = 0$ to $z \sim 1.2$, remains flat to $z \sim 2.5$–3.0 followed by a decrease at higher redshifts and reaches the same level at $z \sim 5$–6 as is measured locally if we assume no variations in this trend.

So, the SFRD and A_{FUV} do not exactly follow the same trends as seen in Figure 2 and Figure 3. The peak of the dust attenuation is delayed with respect to the plateau of the total SFRD by about 3 Gyrs. To better understand the delay, it is necessary to perform an analysis via models that are fed with data of the gas content and the metallicity evolution. Also, a deeper analysis of the dust and metallicity characteristics of these galaxies would provide some insight on the origin of this delay. *SPICA*/SAFARI spectroscopy is probably the best instrument that could be used to carry out this work.

Figures 2 and 3 taken together at face value would suggest that the universe's dusty era (meaning dust attenuation higher than in the local universe) started at $z = 3$–4 simultaneously with the rise of a universe-wide star-formation event.

Figure 3 allowed us to follow the SFRD over most of the Hubble time in a consistent way. However, large uncertainties prevented us from closing the case. To go further in redshift, we need to detect and characterize galaxies at higher redshifts. This means better sensitivities and redshift measurements. *SPICA* spectroscopy and *SPICA*/Mid-IR instrument are best suited to extend the present work to much higher redshift.

This work is further detailed in Burgarella et al. (2013).

REFERENCES

Barger, A. J., et al. 2012, ApJ, 761, 89

Dust Attenuation and Star Formation Histories at High Redshift

Behroozi, P. S., Wechsler, R. H., & Conroy, C. 2012, ApJ, 770, 57

Bouwens, R. J., et al. 2009, ApJ, 705, 936

Buat, V., et al. 2009, A&A, 507, 693

Burgarella, D., Buat, V., Gruppioni, C., et al. 2013, A&A, 554, 70

Burgarella, D., et al. 2005, MNRAS, 360, 1413

Chary, R., & Elbaz, D. 2001, A&A, 556, 562

Cucciati, O., et al. 2012, A&A, 539, 31

Dwek, E., & Cherchneff, I. 2011, ApJ, 727, 63

Franceschini, A., et al. 2010, A&A, 517, 74

Goto, T., et al. 2010, A&A, 514, 6

Gruppioni, C., et al. 2013, MNRAS, 432, 23

Hopkins, P. F., & Beacom, J. 2006, ApJ, 651, 142

Le Floc'h, E., et al. 2005, ApJ, 632, L169

Lutz, D., et al. 2011, A&A, 532, L90

Magnelli, B., et al. 2012, A&A, 539, 155

Oliver, S. J., et al. 2012, MNRAS, 424, 1614

Takeuchi, T. T., Buat, V., & Burgarella, D. 2005, A&A, 440, L17

Valiante, R., Schneider, R., Bianchi, S., & Andersen, A. J. 2009, MNRAS, 397, 1661